Electronic Supplementary Material (ESI) for Journal of Materials Chemistry A.
This journal is © The Royal Society of Chemistry 2020

Electronic supplementary information (ESI)

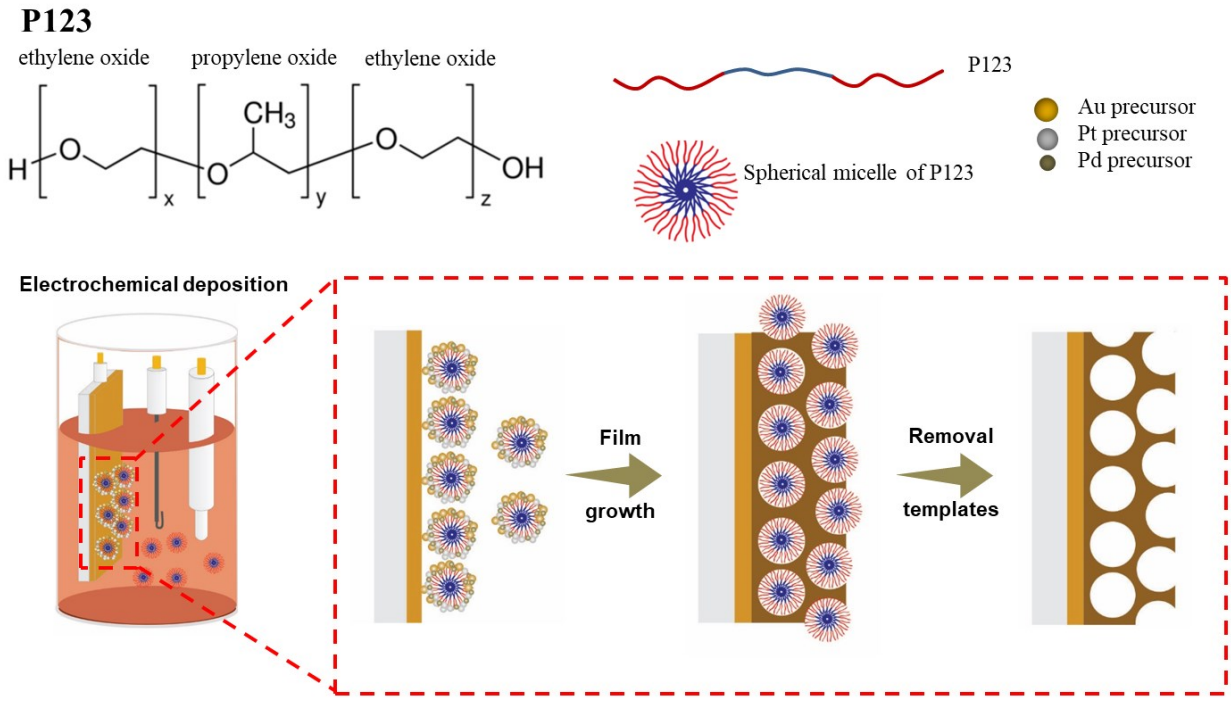

Figure S1. Schematic of fabrication of mesoporous PtPdAu alloy film by electrochemical deposition with the micelle assembly approach.

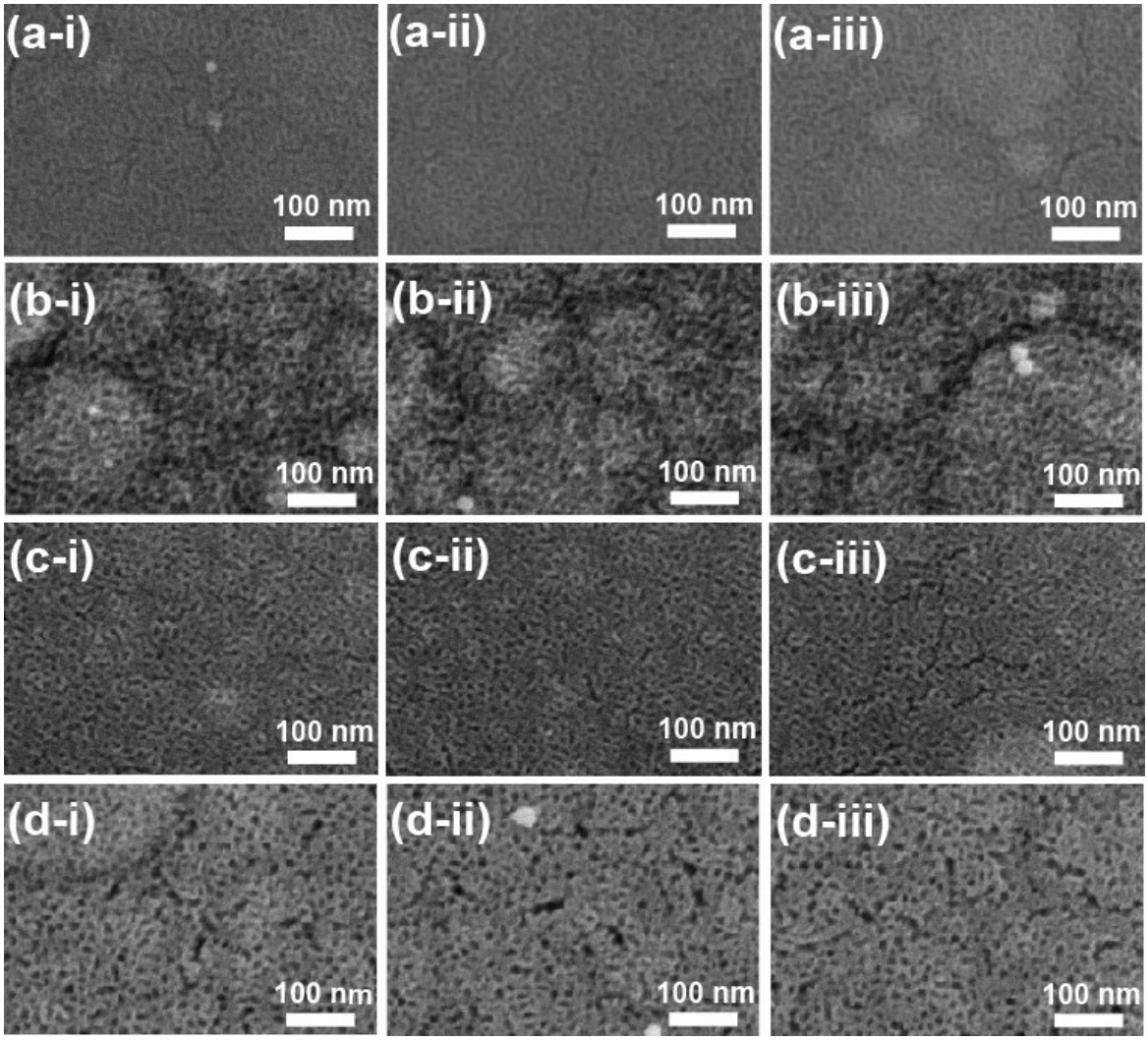

Figure S2. Top-view SEM images from 3 different samples (i, ii,and iii) of selected mesoporous PtPdAu films in the initial dataset with the chemical compositions of metal precursors $[PtCl_4]^{2-}$: $[PdCl_4]^{2-}$: $[AuCl_4]^-$ of (a) 40: 40: 20, (b) 20: 40: 40, (c) 60: 30: 10, and (d) 30: 10: 60.

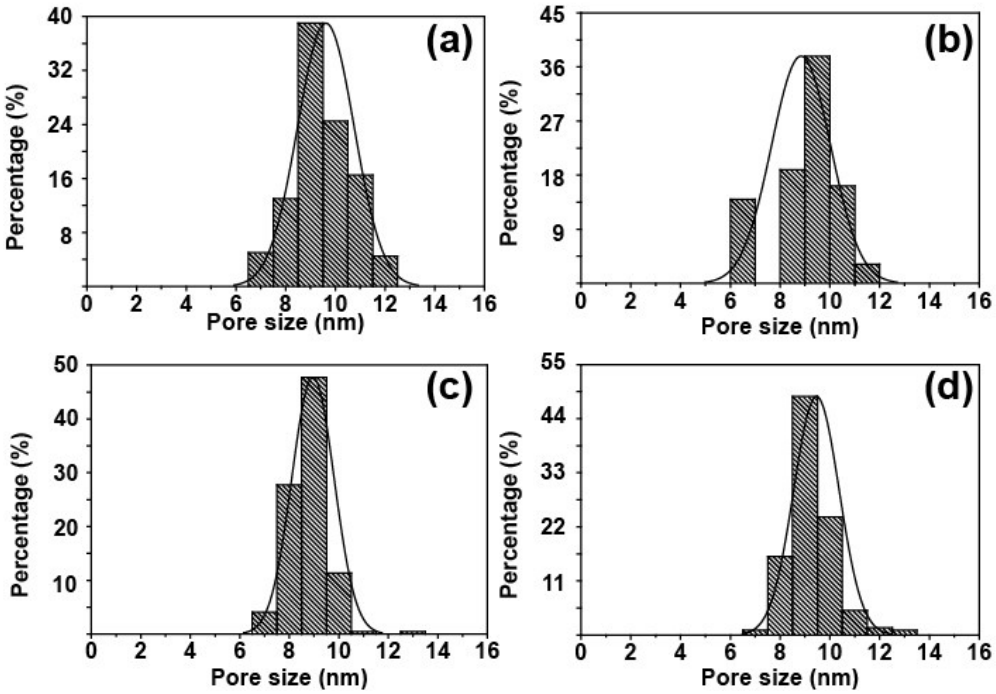

Figure S3. Mesopore size distribution of selected mesoporous PtPdAu films in the initial dataset with the chemical compositions of metal precursors $[PtCl_4]^{2-}$: $[PdCl_4]^{2-}$: $[AuCl_4]^-$ of (a) 40: 40: 20, (b) 20: 40: 40, (c) 60: 30: 10, and (d) 30: 10: 60. Pore size distribution was taken from 3 samples for each condition with minimum 200 pores were measured.

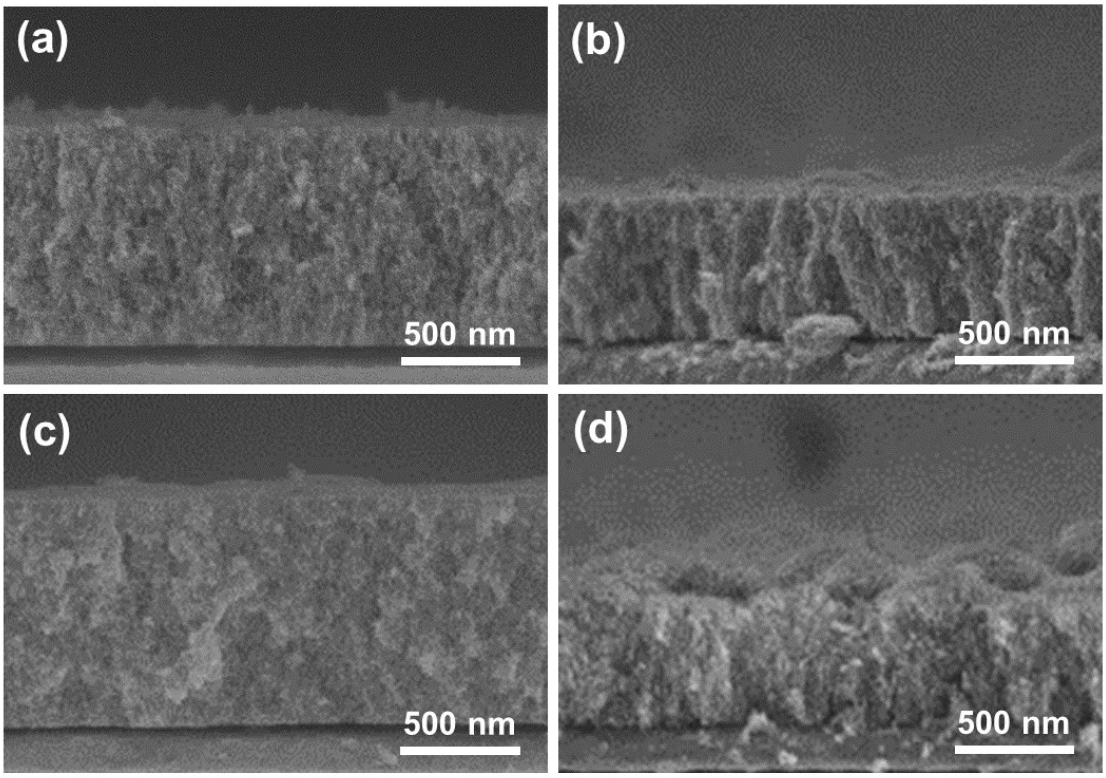

Figure S4. Cross-sectional view SEM images of selected mesoporous PtPdAu films in the initial dataset with the chemical compositions of metal precursors $[PtCl_4]^{2-}$: $[PdCl_4]^{2-}$: $[AuCl_4]^-$ of (a) 40: 40: 20, (b) 20: 40: 40, (c) 60: 30: 10, and (d) 30: 10: 60.

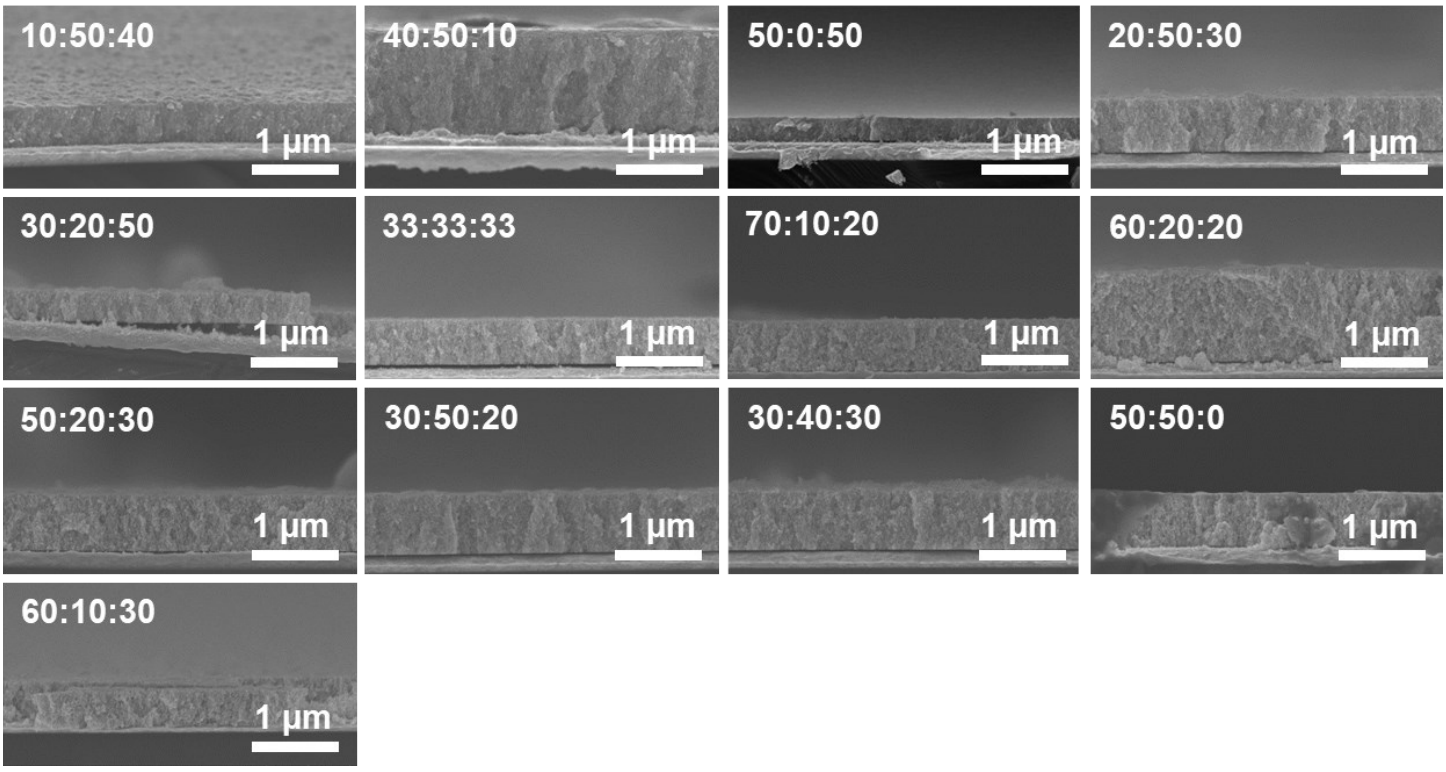

Figure S5. Cross-section SEM images of mesoporous PtPdAu produced by different compositional ratios of the precursor Pt:Pd:Au in the initial dataset. $[PtCl_4]^{2-}$:$[PdCl_4]^{2-}$:$[AuCl_4]^{-}$ ratio in the initial electrolyte solution.

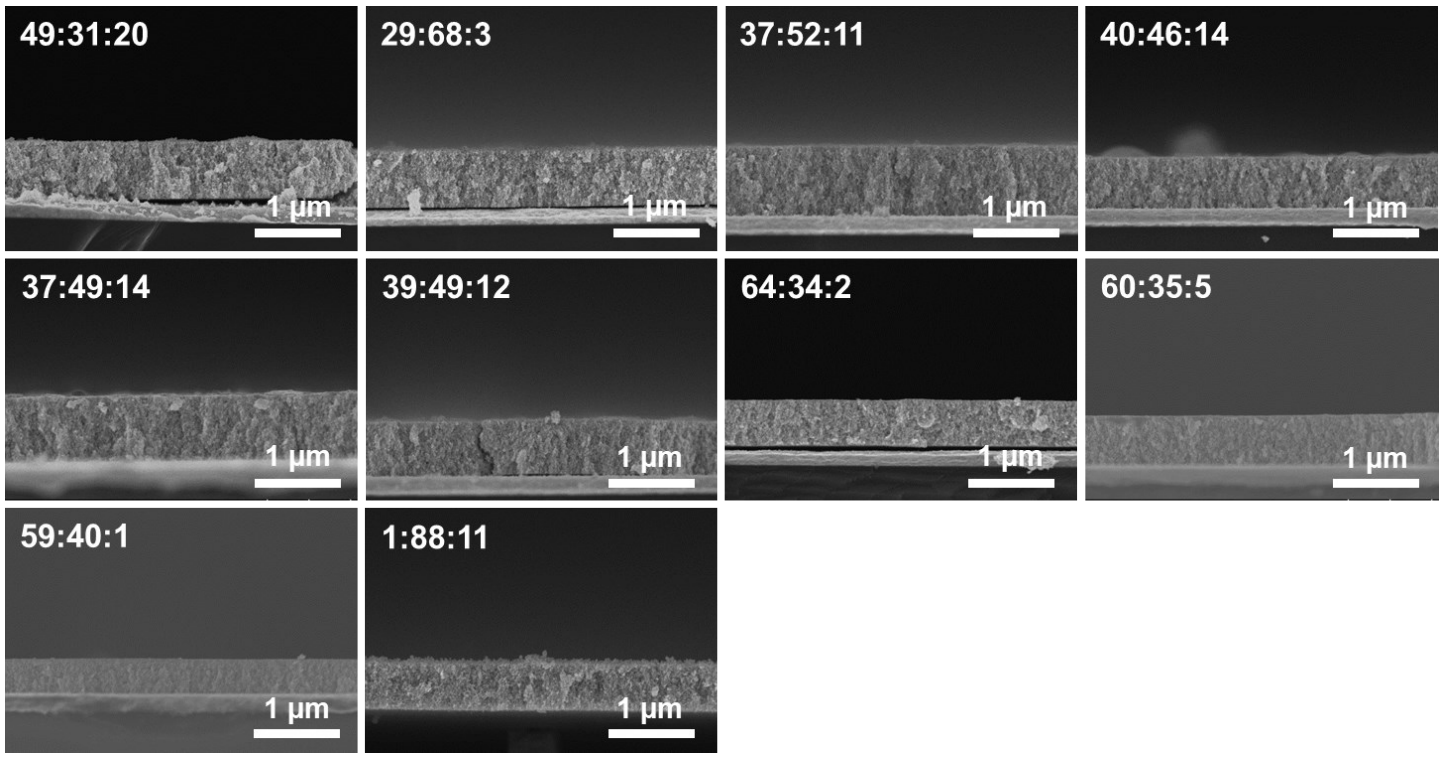

Figure S6. Cross-section SEM images of mesoporous PtPdAu produced by different compositional ratios of the precursor Pt:Pd:Au (dataset from 1st cycle). $[PtCl_4]^{2-}$:$[PdCl_4]^{2-}$:$[AuCl_4]^-$ ratio in the initial electrolyte solution.

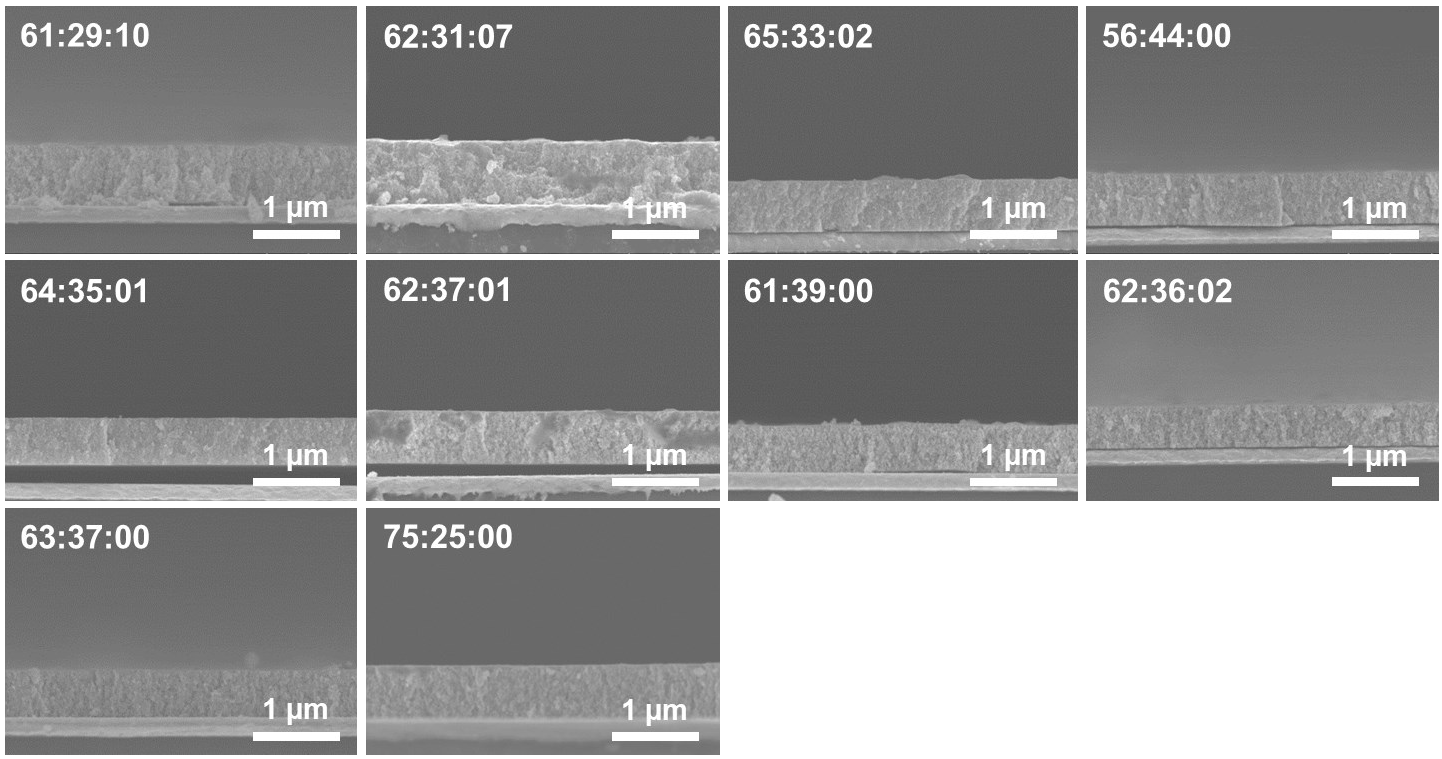

Figure S7. Cross-section SEM images of mesoporous PtPdAu produced by different compositional ratios of the precursor Pt:Pd:Au (dataset from 2nd cycle). $[PtCl_4]^{2-}$:$[PdCl_4]^{2-}$:$[AuCl_4]^-$ ratio in the initial electrolyte solution.

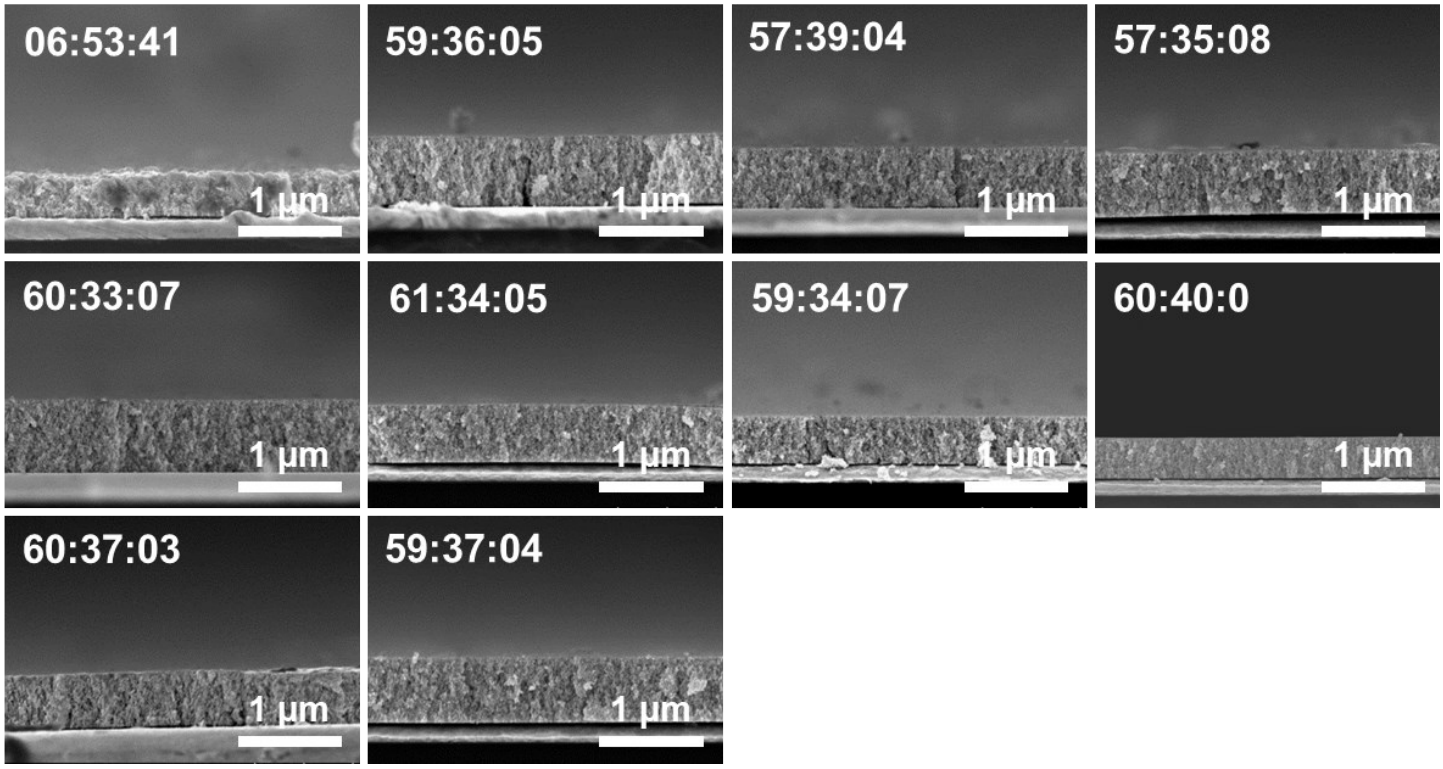

Figure S8. Cross-section SEM images of mesoporous PtPdAu produced by different compositional ratios of the precursor Pt:Pd:Au (dataset from 3rd cycle). $[PtCl_4]^{2-}$:$[PdCl_4]^{2-}$:$[AuCl_4]^-$ ratio in the initial electrolyte solution.

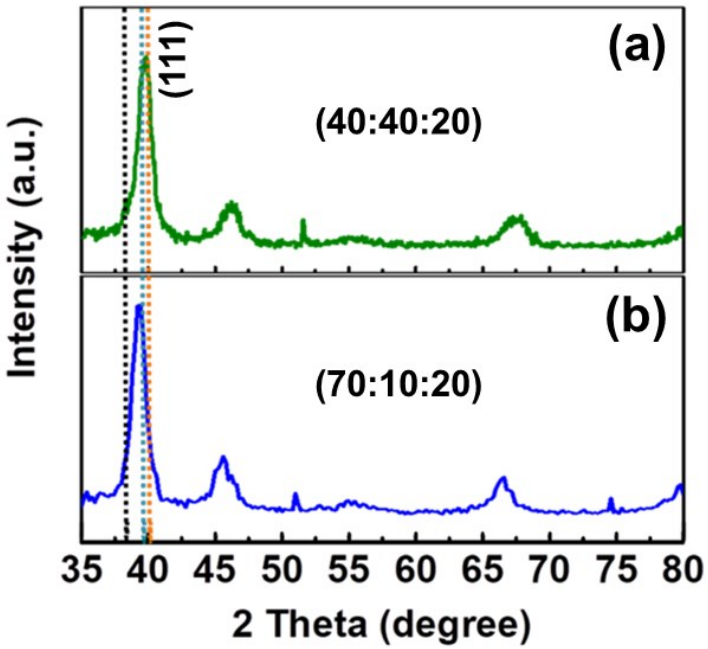

Figure S9. Wide-angle XRD patterns of selected mesoporous PtPdAu films in the initial dataset with the chemical compositions of metal precursors $[PtCl_4]^{2-}$: $[PdCl_4]^{2-}$: $[AuCl_4]^-$ of (a) 40:40:20 and (b) 70:10:20. Dot lines represent: *fcc* Pt (JCPDS 05-0682), light blue; *fcc* Pd (JCPDS 04-0802), orange; *fcc* Au (JCPDS 04-0784), black.

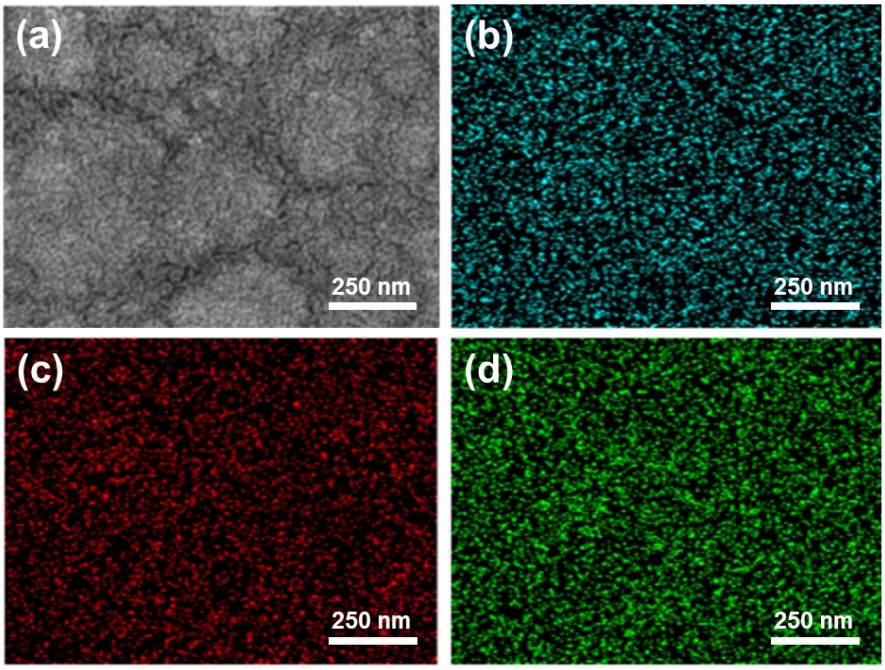

Figure S10. (a) Top-view SEM image and the corresponding EDX elemental mapping (b) Au, (c) Pd, and (d) Pt of mesoporous PtPdAu film fabricated from the electrolyte solution with chemical composition of $[PtCl_4]^{2-}$: $[PdCl_4]^{2-}$: $[AuCl_4]^-$ of 33: 33: 33.

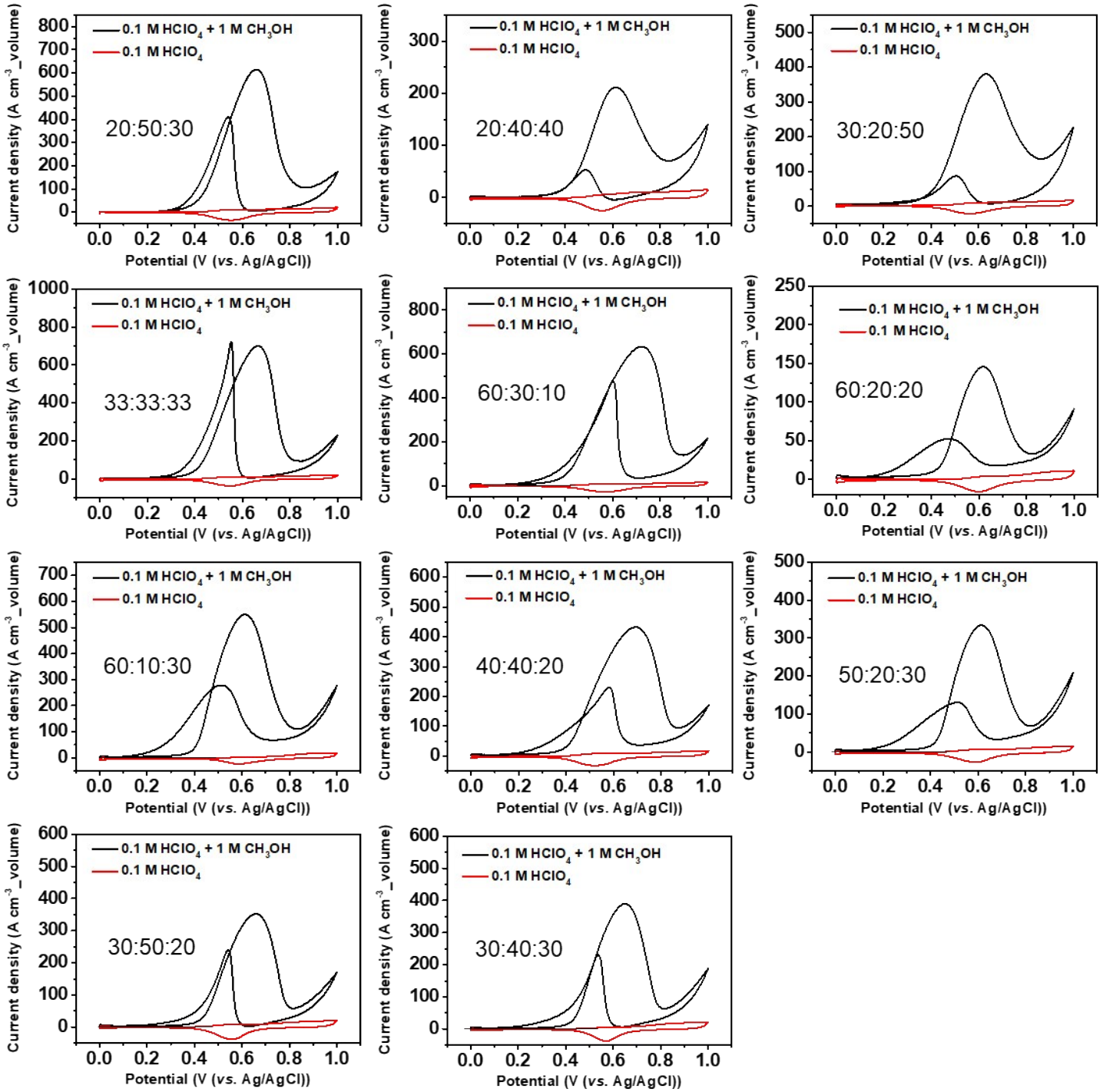

Figure S11. Cyclic voltammetry curves of methanol electrooxidation in 0.1 M $HClO_4$ + 1 M CH_3OH at the scan rate of 5 mV s^{-1} using mesoporous PtPdAu films in the initial dataset. The current density is normalized by the film volume.

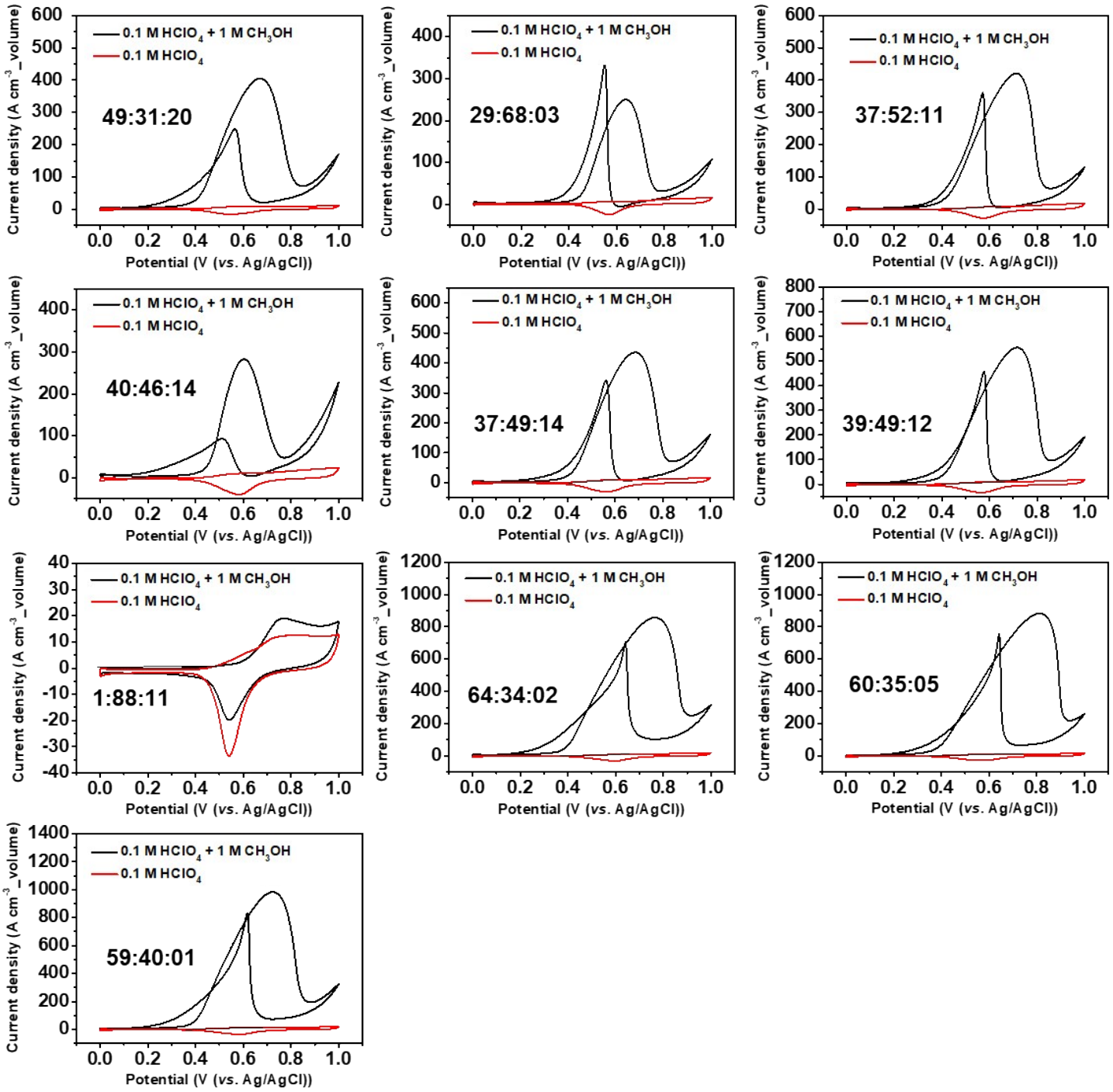

Figure S12. Electrocatalytic performance of mesoporous PtPdPAu with different compositions (dataset from 1st cycle) on MOR in 0.1 M $HClO_4$ + 1 M methanol at scan rate of 5 mV s^{-1}. $[PtCl_4]^{2-}$:$[PdCl_4]^{2-}$:$[AuCl_4]^-$ ratio in the initial electrolyte solution.

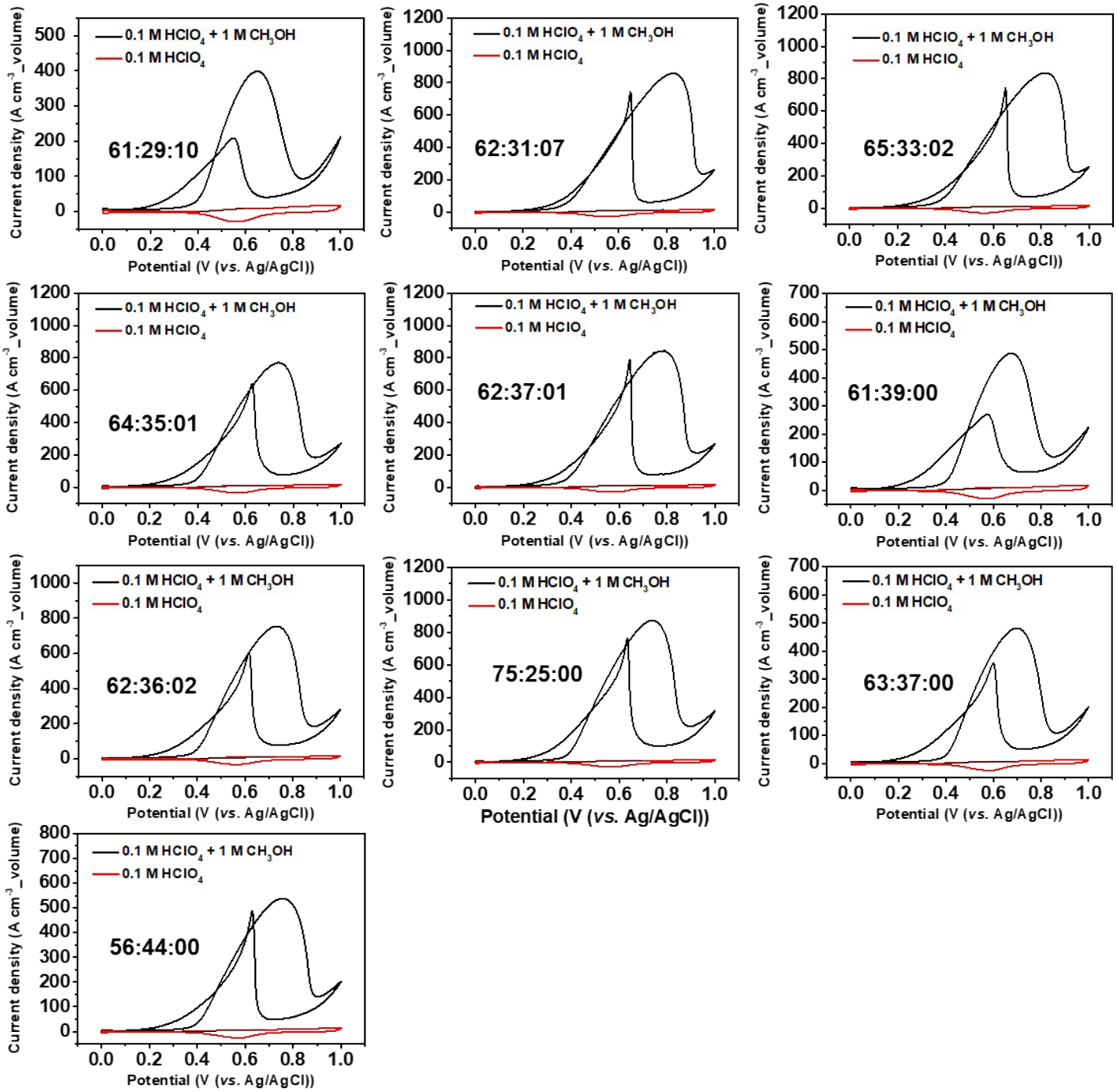

Figure S13. Electrocatalytic performance of mesoporous PtPdPAu with different compositions (dataset from 2nd cycle) on MOR in 0.1 M $HClO_4$ + 1 M methanol at scan rate of 5 mV s^{-1}. $[PtCl_4]^{2-}$:$[PdCl_4]^{2-}$:$[AuCl_4]^-$ ratio in the initial electrolyte solution.

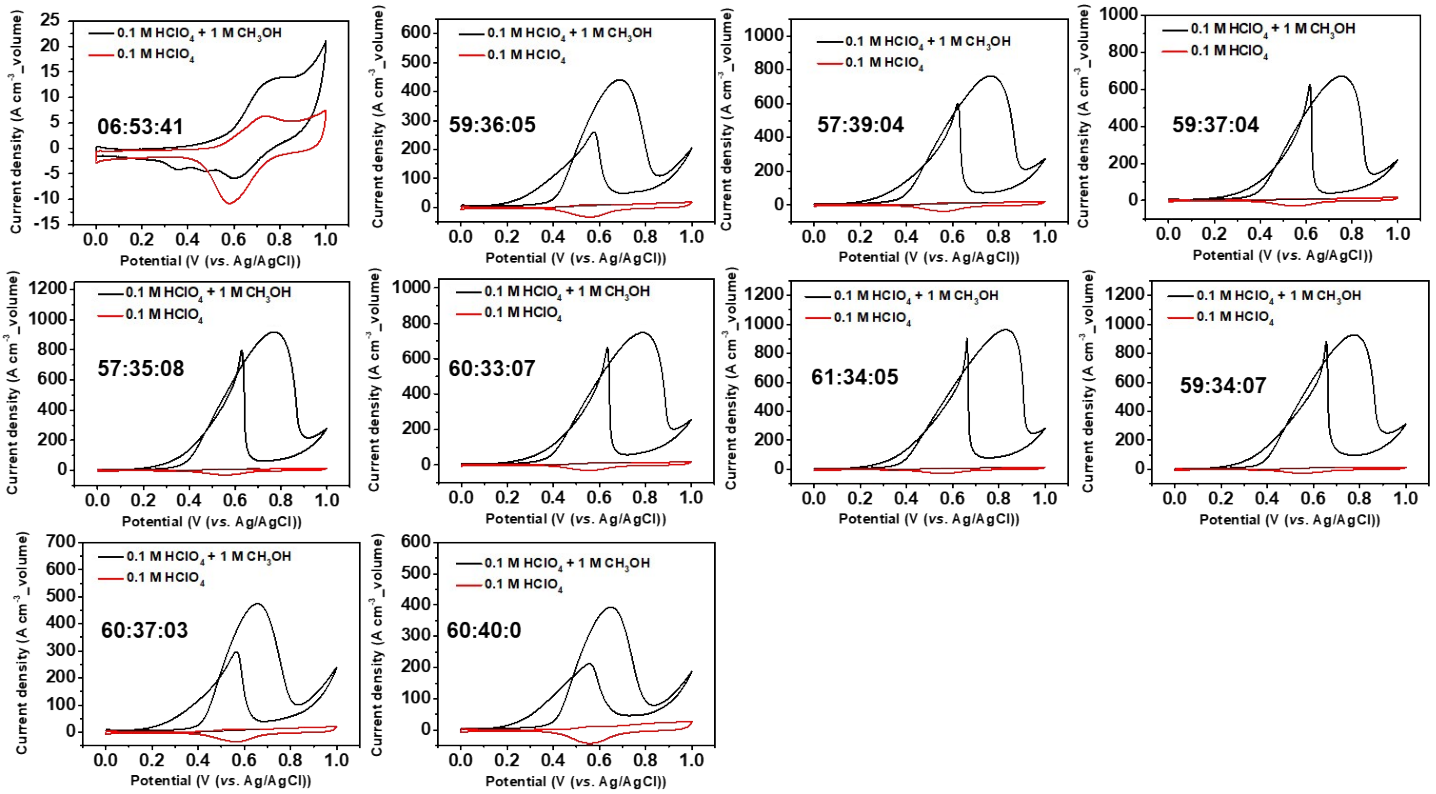

Figure S14. Electrocatalytic performance of mesoporous PtPdPAu with different compositions (dataset from 3rd cycle) on MOR in 0.1 M $HClO_4$ + 1 M methanol at scan rate of 5 mV s^{-1}. $[PtCl_4]^{2-}$:$[PdCl_4]^{2-}$:$[AuCl_4]^-$ ratio in the initial electrolyte solution.

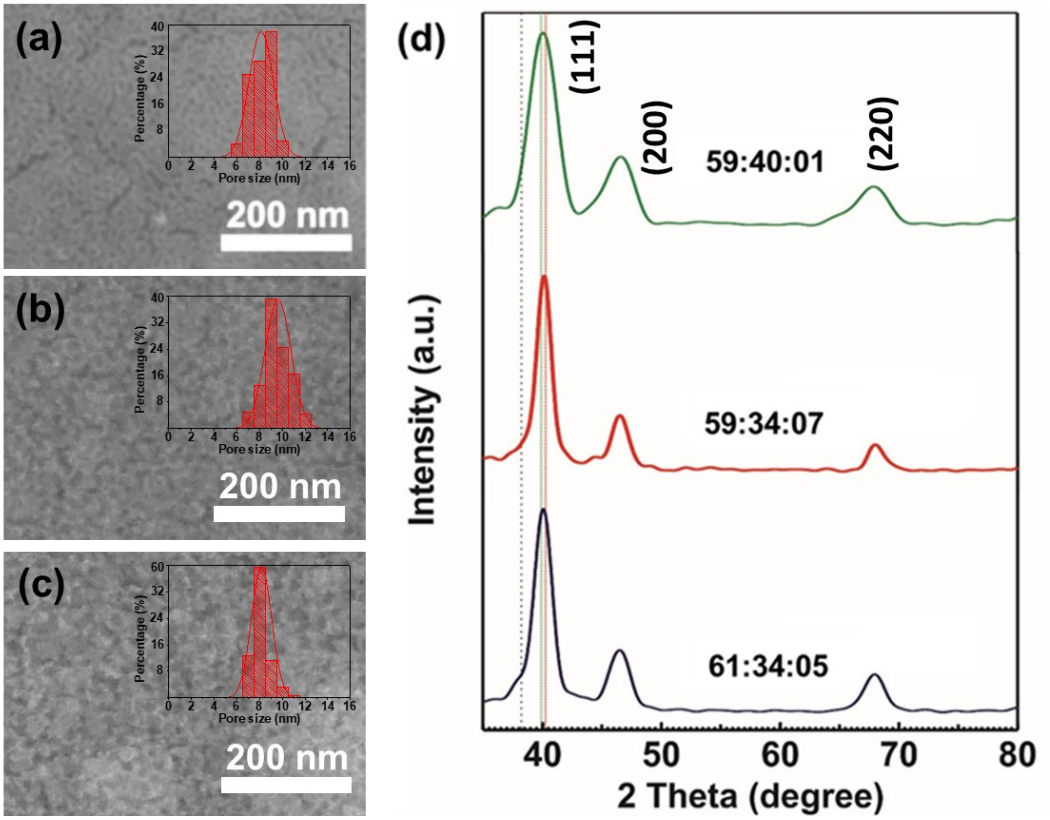

Figure S15. Top-view SEM images of mesoporous PtPdAu films fabricated from electrolyte solutions with $[PtCl_4]^{2-}$: $[PdCl_4]^{2-}$: $[AuCl_4]^-$ of (a) 59: 40: 1, (b) 59: 34: 7, and (c) 61: 34: 5. (d) Wide-angle XRD patterns of mesoporous PtPdAu films. Dot lines represent: *fcc* Pt (JCPDS 05-0682), light blue; *fcc* Pd (JCPDS 04-0802), orange; *fcc* Au (JCPDS 04-0784), black.

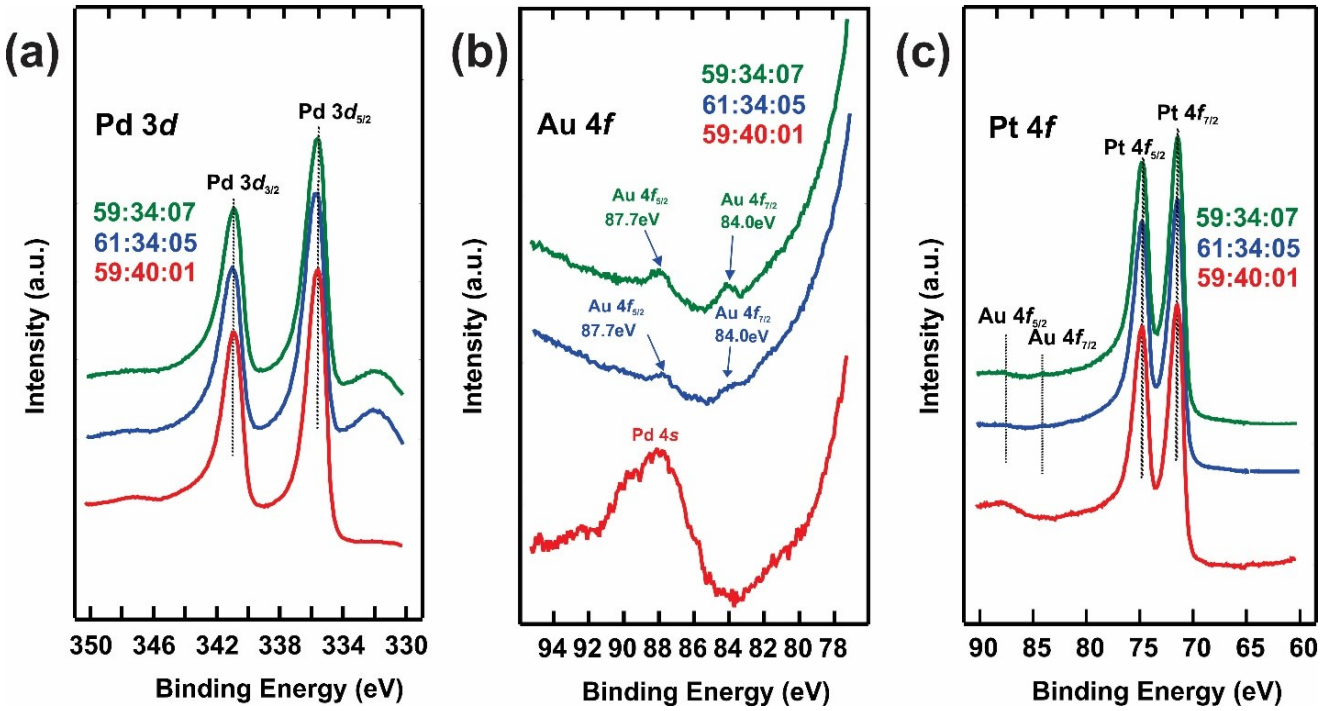

Figure S16. XPS spectra of mesoporous PtPdAu films fabricated from electrolyte solutions with $[PtCl_4]^{2-}$: $[PdCl_4]^{2-}$: $[AuCl_4]^-$ of 59: 40: 1 (red line), 61: 34: 5 (blue line) and 59: 34: 7 (green line) on (a) Pd 3*d*, (b) Au 4*f*, and (c) Pt 4*f*.

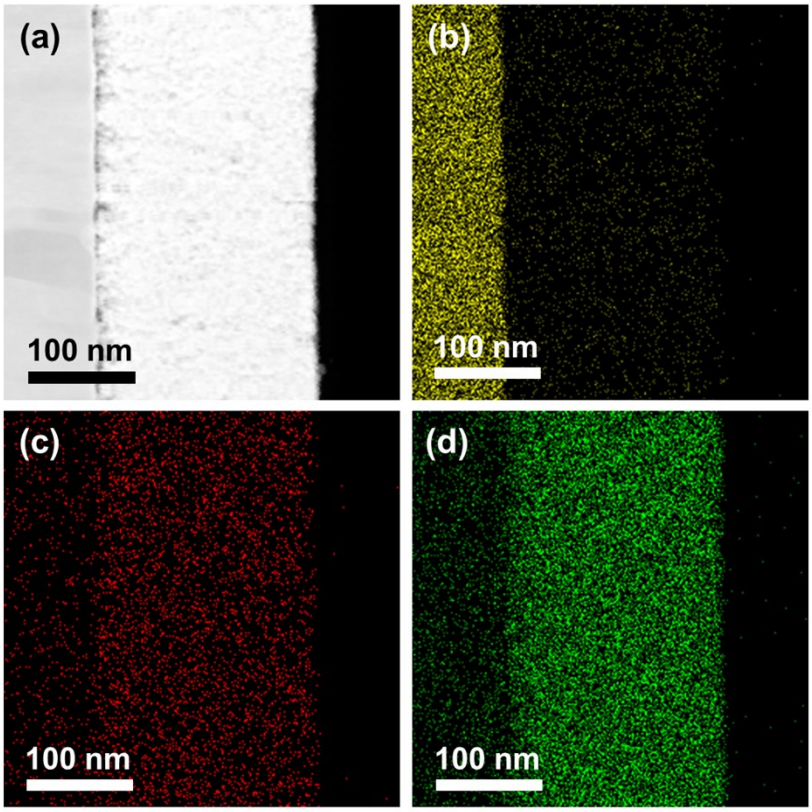

Figure S17. (a) HAADF-STEM image and the corresponding EDX elemental mapping of (b) Au, (c) Pd, and (d) Pt of mesoporous PtPdAu film fabricated from the electrolyte solution with $[PtCl_4]^{2-}$: $[PdCl_4]^{2-}$: $[AuCl_4]^-$ of 59: 40: 1.

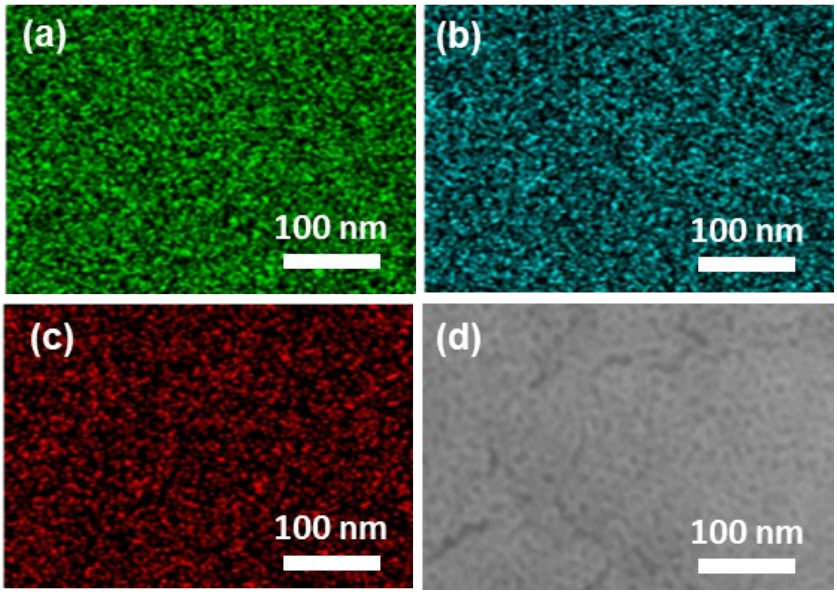

Figure S18. EDX elemental mapping of (a) Pt, (b) Pd, (c) Au, and (d) Top-surface of mesoporous PtPdAu film fabricated from the electrolyte solution with $[PtCl_4]^{2-}$: $[PdCl_4]^{2-}$: $[AuCl_4]^-$ of 59: 40: 1.

Table S1. Compositional ratios of metal precursors in the electrolyte solutions, and thickness and electrocatalytic results on methanol oxidation of the resulting films.[a]

Run	Compositions of metal precursors (Pt: Pd: Au)[b]	Film thickness [nm]	Onset potential[c] [V]	Peak potential[c] [V]	Peak current volume density [A cm^{-3}]
			Initial dataset		
1	10: 50: 40	467	0.42	0.64	35.76
2	30: 10: 60	407	0.41	0.61	227.03
3	20: 50: 30	632	0.42	0.65	618.67
4	20: 40: 40	636	0.43	0.61	212.26
5	30: 20: 50	364	0.42	0.63	381.87
6	33: 33: 33	559	0.42	0.66	701.79
7	50: 0: 50	333	0.44	0.55	79.58
8	70: 10: 20	602	0.41	0.61	468.44
9	60: 30: 10	975	0.41	0.72	633.85
10	60: 20: 20	1110	0.43	0.62	145.95
11	60: 10: 30	449	0.40	0.61	550.11
12	40: 40: 20	923	0.40	0.70	433.37
13	40: 50: 10	1267	0.39	0.72	511.44
14	50: 20: 30	703	0.42	0.61	334.28
15	30: 50: 20	720	0.43	0.66	352.78
16	30: 40: 30	703	0.43	0.65	389.76
17	50: 50: 0	661	0.44	0.62	338.88
			Dataset from 1st cycle		
18	49: 31: 20	728	0.41	0.67	405.32
19	29: 68: 3	677	0.45	0.64	250.01
20	37: 52: 11	838	0.42	0.71	420.31
21	40: 46: 14	635	0.46	0.60	284.05
22	37: 49: 14	847	0.42	0.68	437.89
23	39: 49: 12	677	0.41	0.71	556.92
24	1: 88: 11	610	n.a.[d]	n.a.[d]	n.a.[d]
25	64: 34: 2	567	0.39	0.76	858.32

26	60: 35: 5	670	0.38	0.81	885.85
27	59: 40: 1	457	0.39	0.72	983.47
		Dataset from 2nd cycle			
28	61: 29: 10	711	0.40	0.65	399.02
29	62: 31: 7	720	0.36	0.83	863.68
30	65: 33: 2	618	0.37	0.82	842.02
31	64: 35: 1	576	0.38	0.74	769.66
32	62: 37: 1	635	0.375	0.79	843.83
33	61: 39: 0	533	0.40	0.67	488.50
34	62: 36: 2	508	0.39	0.73	757.66
35	75: 25: 0	449	0.39	0.74	879.32
36	63: 37: 0	584	0.39	0.69	481.99
37	56: 44: 0	627	0.38	0.76	540.94
		Dataset from 3rd cycle			
38	6: 53: 41	452	n.a.[d]	n.a.[d]	n.a.[d]
39	59: 36: 5	676	0.40	0.69	441.05
40	57: 39: 4	611	0.38	0.69	767.41
41	59: 37: 4	660	0.38	0.76	671.42
42	57: 35: 8	647	0.38	0.75	921.06
43	60: 33: 7	726	0.37	0.77	751.96
44	61: 34: 5	597	0.38	0.79	968.73
45	59: 34: 7	503	0.38	0.83	929.33
46	60: 37: 3	561	0.41	0.65	475.34
47	60: 40: 0	483	0.41	0.65	392.61

[a]Electrochemical oxidation of methanol was measured in 0.1 M $HClO_4$ containing 1.0 M CH_3OH.

[b]Molar ratios of $[PtCl_4]^{2-}$:$[PdCl_4]^{2-}$:$[AuCl_4]^-$ in the electrolyte solutions.

[c]Reported with Ag/AgCl reference.

[d]Oxidation peak was too small to accurately determine the values (i.e., almost no activity).